Minimal entangled states and modular matrix for fractional quantum Hall effect in topological flat bands

W. Zhu, D. N. Sheng, and F. D. M. Haldane

Phys. Rev. B **88**, 035122 — Published 17 July 2013

DOI: 10.1103/PhysRevB.88.035122

Minimal Entangled States and Modular Matrix for Fractional Quantum Hall Effect in Topological Flat Bands

W. Zhu[1], D. N. Sheng[1], F. D. M. Haldane[2]
[1]*Department of Physics and Astronomy, California State University, Northridge, California 91330, USA and*
[2]*Department of Physics, Princeton University, Princeton, NJ 08544, USA*

We perform an exact diagonalization study of the topological order in topological flat band models through calculating entanglement entropy and spectra of low energy states. We identify multiple independent minimal entangled states, which form a set of orthogonal basis states for the groundstate manifold. We extract the modular transformation matrices $\mathcal{S}$ ($\mathcal{U}$) which contains the information of mutual (self) statistics, quantum dimensions and fusion rule of quasiparticles. Moreover, we demonstrate that these matrices are robust and universal in the whole topological phase against different perturbations until the quantum phase transition takes place.

PACS numbers: 73.43.Cd,03.65.Ud,05.30.Pr

I. INTRODUCTION

The fractional quantum Hall (FQH) state is the best-known many-body state with topological order discovered in 2D electron systems under strong magnetic field. The most striking features of FQH state are the topological ground state degeneracy on torus and the emerging quasiparticles obeying fractional statistics[1,2]. Recently, it has been demonstrated that FQH states can also be realized in various topological flat-band (TFB) models without Landau levels[3–21]. In such an interacting system, an explicit demonstration of topological order and quasiparticle statistics is still highly desired, which has attracted lots of recent interests[22–31].

Entanglement measurements such as topological entanglement entropy (TEE)[23,24] and entanglement spectrum[25] have been identified as powerful tools for detecting topological properties of many-body quantum states. Insightfully, Zhang *et al.* proposed to extract modular matrix through the entanglement measurement[28], which encodes the complete information of the topological order including quasiparticles quantum dimension and statistics as first described by Wen[22]. Based on the model wavefunctions for toric code and chiral spin liquid states, they demonstrated that the transformation between the minimal entangled states (MESs) along two interwinding partition directions gives rise to modular matrices. The new route to extract modular matrix through MESs improves the practical implementation for strongly interacting systems as such information is accessible through larger system density matrix renormalization group (DMRG) calculations demonstrated for bosonic FQH state $\nu = 1/2$ in TFB[29] and fermionic FQH states with magnetic field[30]. However, it remains difficult to access multiple low energy states in DMRG in a controlled way, when there are coupling between different topological sectors induced by interaction or when the groundstates have higher degeneracy, which will be the focuses of our exact diagonalization (ED) study.

In this paper, we present an ED calculation for the TFB model and map out the entanglement entropy profile for superposition states of the near degenerating groundstates. We demonstrate that there are the same number of the MESs as the ground state degeneracy for FQH phase on a torus, which form the orthogonal and complete basis states for modular transformation. Through locating the MESs along two interwinding partition directions, we extract the modular matrices $\mathcal{S}$ and $\mathcal{U}$ containing generalized statistics of quasiparticles, which unambiguously demonstrate the fractional quasiparticle statistics in such systems for $\nu = 1/2, \nu = 1/4$ (bosons), and $\nu = 1/3$ (fermions) FQH states, respectively. We also analyze the entanglement spectra and obtain TEE from the difference of the maximum and minimum of entanglement entropies of these superposition states. Furthermore, we study the quantum phase transition from FQH phase to the topological trivial phase driven by the disorder scattering or attractive anisotropic interaction. Significantly, the extracted modular matrices remain to be universal containing the same quasi-particle fractional statistics information as theoretical ones for the model FQH states in the whole topological phase until the quantum phase transition takes place. This is distinctly different from following the Berry phase of the ground states, where only the sum of the total Chern number remains invariant[32] due to the lifting of the degeneracy by perturbations for any finite size systems.

The paper is organized as follows. In Sec. II, we briefly introduce the TFB models and the method for calculation. In Sec. III, we study the structure of MESs in the space of groundstate manifold at filling factor $\nu = 1/2$, $\nu = 1/3$ and $\nu = 1/4$, respectively. In Sec. IV, we extract the modular transformation matrices $\mathcal{S}$ and $\mathcal{U}$ with the help of MESs. In Sec. V, we analyze the entanglement spectra of the maximum and minimum entangled states and calculate the TEE. In Sec. VI, we study the MESs and related quasiparticle statistics when we introduce some perturbations to drive a quantum phase transition. We end the paper with a conclusion in Sec. VII.

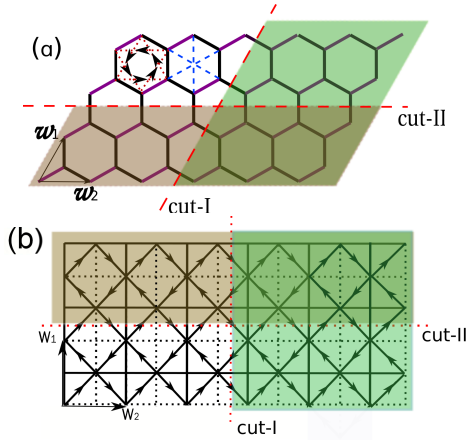

FIG. 1: (Color online) (a) Haldane model on $2\times4\times6$ HC lattice with lattice vectors $\vec{w}_1, \vec{w}_2$. The arrow directions on red dotted lines present the signs of the phases $\pm\phi$ in the NNN hopping terms. The NNNN hoppings are represented by the blue dashed lines. The two ways to bipartition the system along dashed lines are labeled as cut-I and cut-II. (b) Checkboard lattice with basis vectors $\vec{w}_1, \vec{w}_2$. The arrow directions present the signs of the phases $\pm\phi$ in the NN hopping terms. The two ways to partition the system along the dashed lines are labeled as cut-I and cut-II, respectively.

II. MODEL AND METHOD

We study two TFB models in this paper. The first model is the Haldane model[3] on the honeycomb (HC) lattice filled with interacting particles:

$$\begin{aligned} H_{\rm HC} &= -t' \sum_{\langle\langle \mathbf{r}\mathbf{r}'\rangle\rangle} \left[c^\dagger_{\mathbf{r}'} c_{\mathbf{r}} \exp\left(i\phi_{\mathbf{r}'\mathbf{r}}\right) + \text{H.c.}\right] \\ &- t \sum_{\langle \mathbf{r}\mathbf{r}'\rangle} \left[c^\dagger_{\mathbf{r}'} c_{\mathbf{r}} + \text{H.c.}\right] - t'' \sum_{\langle\langle\langle \mathbf{r}\mathbf{r}'\rangle\rangle\rangle} \left[c^\dagger_{\mathbf{r}'} c_{\mathbf{r}} + \text{H.c.}\right] \\ &+ V_1 \sum_{\langle \mathbf{r}\mathbf{r}'\rangle} n_{\mathbf{r}} n_{\mathbf{r}'} + \sum_{\mathbf{r}} \epsilon_{\mathbf{r}} c^\dagger_{\mathbf{r}} c_{\mathbf{r}} \end{aligned} \quad (1)$$

where $c^\dagger_{\mathbf{r}}$ creates a hard-core boson (or fermion) at site $\mathbf{r}$, $n_{\mathbf{r}} = c^\dagger_{\mathbf{r}} c_{\mathbf{r}}$ is the boson (or fermion) number operator. $\langle \ldots \rangle$, $\langle\langle \ldots \rangle\rangle$ and $\langle\langle\langle \ldots \rangle\rangle\rangle$ denote the nearest-neighbor (NN), the next-nearest-neighbor (NNN) and the next-next-nearest-neighbor (NNNN) pairs of sites (Fig. 1 (a)), and V_1 is the NN interaction. The last term models the Anderson on-site disorder $\epsilon_{\mathbf{r}}$ randomly distributed in $[-W, W]$. On the HC lattice, we select the parameters $t = 1$, $t' = 0.60$, $t'' = -0.58$ and the magnitude of the hopping phase $\phi = 0.4\pi$, which lead to a topological flat-band with flatness ratio about 50[8].

The second model is TFB model on checkerboard (CB) lattice[6,8]:

$$\begin{aligned} H_{\rm CB} &= -t \sum_{\langle \mathbf{r}\mathbf{r}'\rangle} \left[c^\dagger_{\mathbf{r}'} c_{\mathbf{r}} \exp\left(i\phi_{\mathbf{r}'\mathbf{r}}\right) + \text{H.c.}\right] \\ &\pm t' \sum_{\langle\langle \mathbf{r}\mathbf{r}'\rangle\rangle} \left[c^\dagger_{\mathbf{r}'} c_{\mathbf{r}} + \text{H.c.}\right] - t'' \sum_{\langle\langle\langle \mathbf{r}\mathbf{r}'\rangle\rangle\rangle} \left[c^\dagger_{\mathbf{r}'} c_{\mathbf{r}} + \text{H.c.}\right] \\ &+ V_1 \sum_{\langle \mathbf{r}\mathbf{r}'\rangle} n_{\mathbf{r}} n_{\mathbf{r}'} \end{aligned} \quad (2)$$

We adopt the parameters $t = -1$, $t' = 1/(2+\sqrt{2})$, $t'' = -1/(2+2\sqrt{2})$ and $\phi = \pi/4$, which leads to a TFB with the flatness ratio about 30.

We consider a finite system of $N_1 \times N_2$ unit cells (total number of sites $N_s = 2\times N_1 \times N_2$) with periodic boundary conditions. The filling factor is $\nu = N_p/(N_1 N_2)$, where N_p is the number of particles. We denote the momentum vector $(2\pi k_1/N_1, 2\pi k_2/N_2)$ with (k_1, k_2) as integer quantum numbers. The groundstates are obtained by the ED method[7,8].

The entanglement entropy is defined by partitioning the full system into two subsystems A and B. Tracing out the subsystem B, one can obtain the reduced density matrix of subsystem A: $\rho_A = tr_B |\Phi><\Phi|$, where $|\Phi>$ is the ground state of the full system. The Renyi $n = 2$ entanglement entropy is defined as: $S = -\log tr\rho_A^2$. (We also confirm the different definition of entropy, von Neumann entropy $S = -Tr\rho_A \log \rho_A$, will not change the parameters of MESs and modular matrices obtained below.) Here we focus on two noncontractible bipartitions on a torus, as shown in Fig. 1 as cut-I and cut-II, respectively.

III. MULTIPLE MESS AS SUPERPOSITIONS OF NEAR DEGENERATING GROUNDSTATES

In TFB lattice model, it has been identified that there are m near degenerating groundstates at filling factor $\nu = 1/m$[7,8] when the interacting system realizes a FQH phase. Here, we try to search the MESs in groundstate manifold for different filling factors.

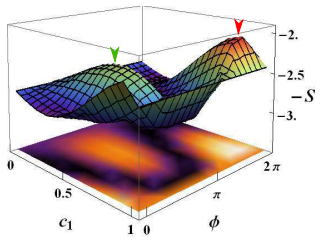

FIG. 2: (Color online) Surface and contour plots of Renyi $n = 2$ entanglement entropy $(-S)$ of wavefunction $|\Phi_{c_1,\phi}>$ on $2\times4\times4$ HC lattice filled with 8 hard-core bosons. The two MESs are labeled by arrows.

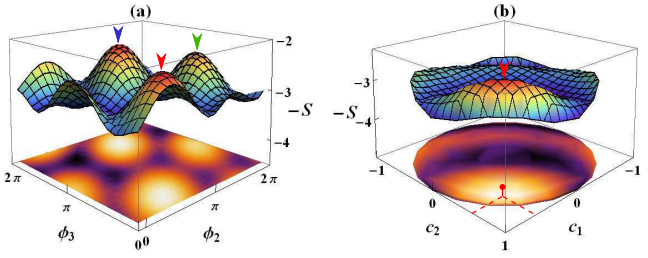

FIG. 3: (Color online) Surface and contour plots of Renyi $n = 2$ entanglement entropy $(-S)$ of wavefunction $|\Psi_{c_1,c_2,\phi_2,\phi_3}>$ on $2\times4\times6$ HC lattice filled with 8 fermions. (a) The entropy $(-S)$ versus ϕ_2 and ϕ_3 by setting $c_1 = c_2 = c_3 = \frac{1}{\sqrt{3}}$. The three MESs are labeled by arrows. (b) The entropy $(-S)$ versus c_1 and c_2 by setting $\phi_2 = 0.546\pi$, $\phi_3 = 0.286\pi$ (the phase parameters for the MES labeled by red arrow in (a)).

A. Filling factor $\nu = 1/2$

Let us first consider a $2\times4\times4$ HC lattice filled with hard-core bosons at half-filling[8]. We set the NN interaction to be zero since hard-core bosons are intrinsically interacting. From ED calculation, we find the two groundstates $|\xi_1>$ and $|\xi_2>$ both in the same momentum sector $(k_1, k_2) = (0, 0)$. This is the general case as long as the two system lengths N_1 and N_2 are factors of the particle number N_p. Now we form the general superposition state as,

$$|\Phi_{c_1,\phi}>= c_1|\xi_1> +c_2e^{i\phi}|\xi_2>$$

where c_1 and ϕ are the real parameter and the relative phase of the state respectively, while $c_2 = \sqrt{1-c_1^2}$. For each state $|\Phi_{c_1,\phi}>$, we construct the reduced density matrix and obtain the corresponding entanglement entropy. In Fig. 2, we draw the $-S$ in the surface and contour plots so that the peaks in entropy show up clearly representing the minimums of S. We identify two peak structures in (c_1, ϕ) parameter space corresponding to two independent MESs:

$$\begin{aligned} |\Xi_1^I> &= 0.892|\xi_1> +0.451e^{i1.74\pi}|\xi_2> \\ |\Xi_2^I> &= 0.455|\xi_1> +0.890e^{i0.74\pi}|\xi_2> \end{aligned} \qquad (3)$$

The minimal entropies at the two peaks are different with $S = 2.044$ and 2.388 respectively, indicating the finite size effect. However, we find the relative phase difference between the two MESs is $\phi(1) - \phi(2) = \pi$ and consequently the two MESs are approximately orthogonal to each other: $|<\Xi_1|\Xi_2>| \approx 0.005$. Due to the $\pi/3$ rotation symmetry in the $2\times4\times4$ system, the MESs along cut-II $|\Xi_i^{II}>$ are related to $|\Xi_i^I>$ as $|\Xi_i^{II}>= R_{\frac{\pi}{3}}|\Xi_i^I>, i = 1, 2$, where $R_{\frac{\pi}{3}}$ is the $\pi/3$ rotation operator.

B. Filling factor $\nu = 1/3$

Now we further examine the relation between the MESs and the degeneracy of the ground state manifold by studying the TFB model filled with fermions at $\nu = 1/3$. We consider a $2\times4\times6$ HC lattice with 8 fermions with repulsive NN $V_1 = 1$ to stabilize the FQH phase[7]. In the ED study, we find three quasi-degenerating groundstates $|\xi_j>$, (with $j = 1, 2, 3$) in momentum sectors $(k_1, k_2) = (0, 0), (0, 2), (0, 4)$, respectively. We search for the superposition states in the space of the groundstate manifold with minimal entropy using the following general wavefunctions:

$$|\Psi_{(c_1,c_2,\phi_2,\phi_3)}>= c_1|\xi_1> +c_2e^{i\phi_2}|\xi_2> +c_3e^{i\phi_3}|\xi_3>$$

where c_1, c_2 are real parameters and ϕ_2, ϕ_3 are relative phases for the state, while c_3 can be obtained using normalization condition. We calculate the entropy of each state $|\Psi_{c_1,c_2,\phi_2,\phi_3}>$ with parameters c_i changing within $[0, 1]$ and ϕ_i within $[0, 2\pi]$. For the bipartition along cut-I, we observe two key points: 1) We can locate three global minimal entropy states in the given parameter space, which always occur when $|c_1| = |c_2| = |c_3| \approx 1/\sqrt{3}$; 2) The relative phases of two different MESs i and j satisfy: $\phi_m(i) - \phi_m(j) \approx \pm\frac{2\pi}{3}$, for $m = 2, 3$. In Fig. 3, we show the surface and contour plots of the entropy of the state $|\Psi_{c_1,c_2,\phi_2,\phi_3}>$ with the optimized parameters for MESs. In Fig. 3(a), we show the entropy of the state $|\Psi_{c_1,c_2,\phi_2,\phi_3}>$ as functions of ϕ_2 and ϕ_3 while other parameters are fixed at $c_1 = c_2 = c_3 = \frac{1}{\sqrt{3}}$. In Fig. 3(b), by fixing the relative phases $\phi_2 = 0.546\pi$ and $\phi_3 = 0.286\pi$, it is found that the $c_1 \approx c_2 \approx c_3$ minimizes the entanglement entropy. We have checked for all other possible ϕ_2 and ϕ_3 and found that the $|c_1| \approx |c_2| \approx |c_3| \approx 1/\sqrt{3}$ indeed minimizes the entanglement entropy. After optimizing the entropy in parameter space $(c_1, c_2, \phi_2, \phi_3)$, we determine the three global MESs as:

$$|\Xi_i^I>= (|\xi_1> +e^{i\phi_2(i)}|\xi_2> +e^{i\phi_3(i)}|\xi_3>)/\sqrt{3} \qquad (4)$$

with state index $i = 1, 2, 3$. We find $(\phi_2(1), \phi_3(1)) = (0.546\pi, 0.286\pi)$, $(\phi_2(2), \phi_3(2)) = (1.220\pi, 1.620\pi)$, $(\phi_2(3), \phi_3(3)) = (1.854\pi, 0.930\pi)$, corresponding to minimum entropies $S = 2.309, 2.309, 2.464$, respectively. Very importantly, the three MESs we found are nearly orthogonal to each other: $|<\Xi_1^I|\Xi_2^I>| \approx 0.007$, $|<\Xi_3^I|\Xi_1^I>| \approx 0.030$ and $|<\Xi_3^I|\Xi_2^I>| \approx 0.025$, which is the necessary condition for these states to form the basis states for modular transformation. The small overlap is a finite size effect as the MESs become the true ground states only in the thermodynamic limit. Since there is no rotation symmetry in $2\times4\times6$ lattice, we separately locate three MESs in the parameter space for the partition along cut-II. Here, we find that each groundstate $|\xi_i>$ is indeed the MES

$$|\Xi_i^{II}>= |\xi_i>, \quad i = 1, 2, 3. \qquad (5)$$

In general, if the groundstates have different momentum quantum number along the entanglement cut direction, any form of mixing groundstates will increase the entropy of the state.

C. Filling factor $\nu = 1/4$

The above results are based on the Haldane model on HC lattice. We also confirm the features of MESs in the groundstate manifold on checkboard (CB) lattice at filling factor $\nu = 1/2$ and $\nu = 1/3$ are similar to the cases on HC lattice. Interestingly, on CB lattice we can identify a four fold degenerating MESs at $\nu = 1/4$ filling corresponding to a FQH $\nu = 1/4$ state[8].

We consider a $2 \times 4 \times 5$ checkboard lattice with five hard-core bosons. In the ED study, the four ground states $|\xi_i>$ $(i = 1, 2, 3, 4)$ lie in momentum sector $(k_1, k_2) = (0, 0)$,$(1, 0)$,$(2, 0)$ and $(3, 0)$, respectively. Now we form the general superposition state from the four quasi-degenerating ground states,

$$|\Psi>= c_1|\xi_1> +c_2e^{i\phi_2}|\xi_2> +c_3e^{i\phi_3}|\xi_3> +c_4e^{i\phi_4}|\xi_4>$$

where c_i are the real parameters and ϕ_i are the relative phase of the state respectively. For the bipartition along cut-I, we find that each groundstate $|\xi_i>$ is indeed the MES due to four ground states having different quantum number k_1 along the cut-I direction:

$$|\Xi_i^I>= |\xi_i>, \;\; i = 1, 2, 3, 4. \tag{6}$$

For the partition along cut-II, it is found that the MESs appear when the four ground states are in equal magnitude superposition: $c_1 = c_2 = c_3 = c_4 = 1/2$. As shown in Fig. 4, we show the entropy of wavefunction $|\Psi>$ in $\phi_2 - \phi_3 - \phi_4$ space by setting $c_1 = c_2 = c_3 = c_4 = 1/2$.

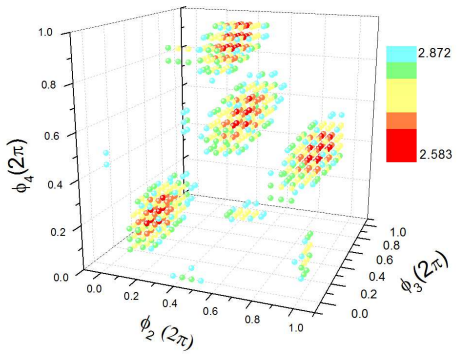

FIG. 4: The entropy of wavefunction $|\Psi>$ on $2\times4\times5$ checkboard lattice with 5 interacting hard-core bosons by setting $c_1 = c_2 = c_3 = c_4 = 1/2$, which is the optimized values for MESs. Here we only show the entropy smaller than 2.872. The calculation is for bipartition system along cut-II direction.

The color of dots represents the magnitude of entropy. For simplicity, we just show the points with entropy smaller than 2.872. It is clear that there exist four valleys in $\phi_2 - \phi_3 - \phi_4$ space. The four valleys corresponding to four independent MESs as:

$$|\Xi_i^{II}>= (|\xi_1> +e^{i\phi_2(i)}|\xi_2> +e^{i\phi_3(i)}|\xi_3> +e^{i\phi_4(i)}|\xi_4>)/2 \tag{7}$$

with state index $i = 1, 2, 3, 4$ and $(\phi_2(1), \phi_3(1), \phi_4(1)) = (0.16\pi, 0.70\pi, 0.26\pi)$, $(\phi_2(2), \phi_3(2), \phi_4(2)) = (0.68\pi, 1.72\pi, 1.76\pi)$, $(\phi_2(3), \phi_3(3), \phi_4(3)) = (1.16\pi, 0.70\pi, 1.26\pi)$, $(\phi_2(4), \phi_3(4), \phi_4(4)) = (1.68\pi, 1.72\pi, 0.76\pi)$, corresponding to minimum entropies $S = 2.592, 2.583, 2.592, 2.583$, respectively. The four MESs are nearly orthogonal to each other: $|<\Xi_1^{II}|\Xi_{2,4}^{II}>| \approx 0.089$, $|<\Xi_1^{II}|\Xi_3^{II}>| \approx 0.0$, $|<\Xi_2^{II}|\Xi_4^{II}>| \approx 0.0$, $|<\Xi_3^{II}|\Xi_{2,4}^{II}>| \approx 0.089$, which forms orthogonal basis states for modular transformation.

IV. MODULAR TRANSFORMATION MATRIX BASED ON MESS

The generalized quasiparticle statistics of a topological ordered state is captured by the modular matrix $\mathcal{S}$ and $\mathcal{U}$ as first proposed by Wen[22]. $\mathcal{S}$ ($\mathcal{U}$) determines the mutual (self) statistics of the different quasiparticles as well as the quantum dimension and fusion rules of quasiparticles[33–35]. In general, the relationship between the modular matrices and MESs is $<\Xi^{II}|\Xi^{I}>= \mathcal{U}^n\mathcal{S}^l\mathcal{U}^m$, where n, m, l are integers determined by specific modular transformation on a lattice[28].

Specially, for a $2\times4\times4$ HC lattice filled with hard-core bosons, the $\pi/3$ rotation symmetry leads to the overlap $<\Xi^{II}|\Xi^{I}>= \mathcal{U}\mathcal{S}^{-1}$[28,29]. Thus by computing the overlap using states from Eq. 3, we obtain,

$$\mathcal{S} \approx 0.722 \begin{pmatrix} 1 & 0.957 \\ 0.957 & -1 \end{pmatrix}, \;\; \mathcal{U} \approx e^{-i\frac{2\pi}{24}0.921} \begin{pmatrix} 1 & 0 \\ 0 & 0.999i \end{pmatrix}$$

which are nearly identical to the theoretical ones[33–35] for the model FQH state: $\mathcal{S} = \frac{1}{\sqrt{2}} \begin{pmatrix} 1 & 1 \\ 1 & -1 \end{pmatrix}$, $\mathcal{U} = e^{-i\frac{2\pi}{24}1} \begin{pmatrix} 1 & 0 \\ 0 & i \end{pmatrix}$. From $\mathcal{S}_{i1} = d_i/D$, we determine the quantum dimension for two type of quasiparticles as $d_1 = 1$,$d_2 \approx 0.957$ and total quantum dimension $D \approx 1.385$ (close to $\sqrt{2}$). $\mathcal{S}_{1i} > 0$ show that one quasiparticle as a boson while $\mathcal{S}_{22} < 0$ indicates another quasiparticle acquires a π phase encircling themselves. Combined with the topological spin $\theta_2 \approx i$ from $\mathcal{U}_{22}$, we identify that these quasiparticles are semions[34].

For $2\times4\times6$ HC lattice filled with interacting fermions, the overlap between Eq. 4 and Eq. 5 gives $<\Xi^{II}|\Xi^{I}>= \mathcal{S}$[28]:

$$\mathcal{S} \approx \frac{1}{\sqrt{3}} \begin{pmatrix} 1 & 1 & 1 \\ 1 & e^{i2\pi\times0.337} & e^{i2\pi\times0.683} \\ 1 & e^{i2\pi\times0.667} & e^{i2\pi\times0.344} \end{pmatrix} \tag{8}$$

TABLE I: The comparison of the calculated TEE $\gamma_{cal} = S_{max} - S_{min}$ (for cut-I) and the theoretical values $\gamma_{Th} = \ln m$ for $1/m$ Laughlin states. HB and FM denote hard-core boson and fermion systems, respectively. HC and CB represent Honeycomb and checkboard lattices. 'Y(N)' means the groundstates have the same (different) momentum.

system	lattice size	GSM	γ_{cal}	γ_{cal}/γ_{Th}
HB on HC $\nu = 1/2$	$2 \times 4 \times 4$	Y	0.849	1.232
HB on HC $\nu = 1/2$	$2 \times 3 \times 6$	N	0.693	0.999
FM on HC $\nu = 1/3$	$2 \times 4 \times 6$	N	1.125	1.024
HB on CB $\nu = 1/2$	$2 \times 4 \times 4$	Y	0.774	1.117
HB on CB $\nu = 1/2$	$2 \times 3 \times 6$	N	0.693	0.999
FM on CB $\nu = 1/3$	$2 \times 4 \times 6$	N	1.128	1.026

The obtained result is close to the analytic prediction[22,34]: $\mathcal{S} = \frac{1}{\sqrt{3}} \begin{pmatrix} 1 & 1 & 1 \\ 1 & \omega & \omega^2 \\ 1 & \omega^2 & \omega \end{pmatrix}$, where $\omega = e^{i\frac{2\pi}{3}}$. The extracted mutual statistics between quasiparticles reflects the Z_3 statistics. The statistics phases are in unit of $2\pi/3$, which clearly signals fractional change $e/3$ of quasiparticles at FQH $\nu = 1/3$ state[1].

Within the same route, we also obtain modular matrix for $\nu = 1/4$ FQH states on CB:

$$\mathcal{S} \approx \frac{1}{2} \begin{pmatrix} 1 & 1 & 1 & 1 \\ 1 & -i & -1 & i \\ 1 & -1 & 1 & -1 \\ 1 & i & -1 & -i \end{pmatrix} + 10^{-2} e^{i0.49\pi} \begin{pmatrix} 0 & 0 & 0 & 0 \\ 0 & 1 & 1 & 0 \\ 0 & 0 & 0 & 0 \\ 0 & 1 & 1 & 0 \end{pmatrix}$$

, which is nearly the same as the one representing Z_4 statistics: $\mathcal{S}_{nn'} = \frac{1}{2} e^{-i\frac{2\pi nn'}{4}}$.

V. TOPOLOGICAL ENTANGLEMENT ENTROPY

For a topological ordered state, one can also identify a topological term in the entanglement entropy since $S = \alpha L - \gamma + \mathcal{O}(L^{-1})$, where L is the length of the smooth boundary between two subsystems and the TEE term is quantized as $\gamma = \log \mathcal{D}$ with $\mathcal{D}$ as the total quantum dimension[23,24]. Recently, it has been shown that TEE of Abelian FQH state can be extracted through[36], $\gamma_{cal} = S_{max} - S_{min}$, where $S_{max(min)}$ is the Renyi $n = 2$ entanglement entropy corresponding to maximal (minimal) entangled state. To check out this relation, the calculated $\gamma_{cal} = S_{max} - S_{min}$ for different systems are shown in Table I. Indeed, the obtained γ_{cal} gives a good estimate of the quantized theoretical value $\gamma_{Th} = 2 \times \ln\sqrt{m} = \ln m$ for $1/m-$Laughlin state on torus[37]. For symmetric system of $2 \times 4 \times 4$ lattice, we obtained a bigger deviation between γ_{cal} and γ_{Th}, which may result from the strong coupling among the groundstates in the same momentum sector. To elucidate the physical difference between minimal and maximal entangled states, we further show entanglement spectra $\{\lambda_i^{max(min)}\}$ of these states in Fig. 5[25,26]. We find that the spectra of the maximal entangled states $\{\lambda_i^{max1(2)}\}$ can be exactly recovered by reducing the density matrix eigenvalues by a factor m ($m = 2$ for $\nu = 1/2$ FQH state) for two sets of spectra of MESs and imposing them on top of each other: $\{\lambda_i^{min1}/m\} \oplus \{\lambda_i^{min2}/m\}$ as shown as cross dots in Fig. 5.

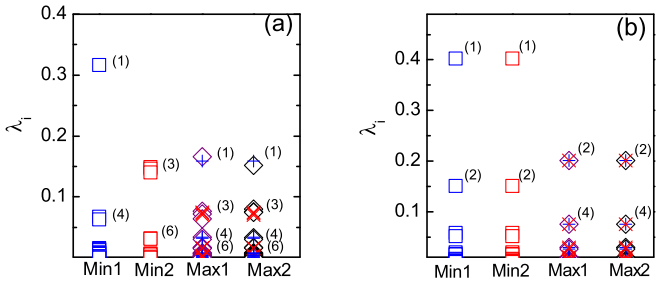

FIG. 5: (Color online) Eigenvalues λ_i of the reduced density matrix of two MESs (square) and two maximal entangled states (diamond) for (a) $2 \times 4 \times 4$ and (b) $2 \times 3 \times 6$ HC lattice with hard-core bosons at $\nu = 1/2$. The number near the dots shows the degeneracy. Crossed blue (purple) dots stand for the combination of $\{\lambda_i^{min1(2)}\}$ as described in the text.

VI. MODULAR MATRIX AND QUANTUM PHASE TRANSITION

Topological order is robust in the presence of any weak local perturbations, which can be used to characterize the topological phase. Here we first consider the disorder effect on bosonic state. As shown in Fig. 6(a-b), the energy spectrum remains two-fold quasi-degenerating protected by a spectrum gap until a disorder strength $W \sim 0.8$. Further calculation of particle entanglement spectrum (PES) reveals a gap at small W and the number of states below this gap agrees with the number of quasihole excitations in a FQH state[9]. This PES gap disappears at $W \sim 0.6$ signaling the quantum phase transition from the FQH phase to a topological trivial state. As shown in Fig. 6(c-d), there are two distinguishable valleys I and II in entropy for the states $|\Phi> = c_1|\xi_1> + c_2 e^{i\phi}|\xi_2>$, and the corresponding MESs are always approximately orthogonal to each other. The modular matrices obtained for an intermediate disorder strength $W = 0.4$ are $\mathcal{S} \approx 0.685 \begin{pmatrix} 1 & 1.109 \\ 1.109 & -0.980 - 0.223i \end{pmatrix}$ and $\mathcal{U} \approx e^{-i\frac{2\pi}{24}1.12} \begin{pmatrix} 1 & 0 \\ 0 & 0.208 + 0.978i \end{pmatrix}$, which remain to be very close to the exact results for bosonic $\nu = 1/2$ Laughlin state. After the quantum phase transition at $W = 0.8$ as shown in Fig. 6(e), there are still two valleys of MESs near $(c_1, \phi) = (0.851, 1.654\pi)$ and $(0.715, 0.684\pi)$, however these two states start to have bigger overlap $|<$

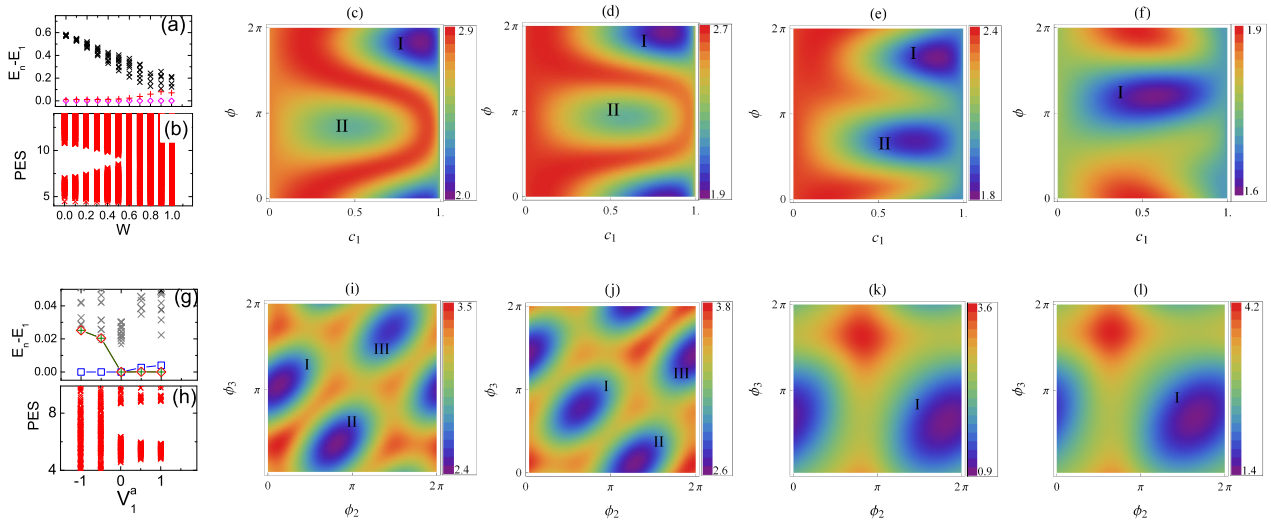

FIG. 6: (Color online) (a-f) Disorder effect on MESs on $2\times4\times4$ HC lattice filled with 8 hard-core bosons. (a) Energy spectrum (two lowest eigenvalues are labeled by diamond and cross) and (b) Particle entanglement spectrum (PES) for tracing out 5 particles. There are 352 states below the PES gap for $W < 0.6$, in good agreement with the counting of quasihole excitations in FQH state. Contour plot of entropy for (c) $W = 0.1$; (d) $W = 0.4$; (e) $W = 0.8$; (f) $W = 1.0$. (g-l) Anisotropic interaction effect on MESs on $2 \times 4 \times 6$ HC lattice filled with 8 fermions. (g) Energy spectrum (three lowest eigenvalues are labeled by blue square, red diamond and green cross) and (h) PES for tracing out 6 particles. There are 228 states below the PES gap for $V_1^a \geq 0$. Contour plot of entropy for (i) $V_1^a = 0.5$; (j) $V_1^a = 0.0$; (k) $V_1^a = -0.5$; (l) $V_1^a = -1.0$. Bipartition are all along cut-I direction.

$\Xi_1|\Xi_2> | \approx 0.245$. The corresponding modular matrix $\mathcal{U}$ and $\mathcal{S}$ are qualitatively different from exact results for $\nu = 1/2$ FQH state as: $\mathcal{S} \approx 0.851 \begin{pmatrix} 1 & 0.636 \\ 0.636 & e^{1.328\pi} \end{pmatrix}$ and $\mathcal{U} \approx \begin{pmatrix} 1 & 0 \\ 0 & 1 \end{pmatrix}$. In particular, the quasi-particle statistics has changed with the $\mathcal{U}$ matrix becomes unit matrix, which indicates we are in a topological trivial phase. At $W = 1.0$ shown in Fig. 6(e), there is only one valley left corresponding to one MES state in parameter space indicating the lost of any feature of topological order.

Furthermore, we consider the effect of the anisotropic interaction for fermionic system by tunning the interaction V_1^a on one NN bond, while keeping the other two at unit strength. Consistent with the geometrical theory of the FQHE[38,39], we find that the topological state and its modular matrix remain to be universal insensitive to the strength of the additional repulsive interactions with no quantum phase transition. So we turn to the additional attractive interaction on one bond. From both energy spectrum and PES, we identify a quantum phase transition which appears between $V_1^a = 0$ and $V_1^a = -0.5$ as shown in Fig. 6(g-h). As shown in Fig. 6(i-l), in the FQH phase, there are three minimal entropy valleys in $\phi_2 - \phi_3$ parameter space while we take $c_1 = c_2 = c_3$, which are the optimized values for all these systems to minimize the entanglement entropy. In FQH phase, the calculated modular matrix is always nearly identical to the expected theoretic result for Laughlin state. Taking $V_1^a = 0.0$ as an example, from the overlap of the MESs we extract $\mathcal{S} \approx \frac{1}{\sqrt{3}} \begin{pmatrix} 1 & 1 & 1 \\ 1 & e^{i2\pi\times0.36} & e^{i2\pi\times0.68} \\ 1 & e^{i2\pi\times0.65} & e^{i2\pi\times0.32} \end{pmatrix}$. After the phase transition occurs (Fig 6(k-l)) at $V_1^a \sim -0.5, -1.0$, we can only locate one minimal entropy valley in $\phi_2 - \phi_3$ parameter space, which demonstrates the disappearance of the FQH phase.

VII. SUMMARY

We study the structure of MESs in the space of the groundstate manifold obtained from ED calculations. By calculating the overlap between different MESs, we obtain modular matrices for different FQH systems. The obtained $\mathcal{S}$ and $\mathcal{U}$ matrices faithfully represent the quasiparticle dimension and fractional statistics for systems with anisotropic interactions and random disorder scattering until a quantum phase transition takes place. We conclude that extracting the quasiparticle statistics information from MESs provides a practical way to investigate and analyze topological order. We will explore the relationship between MES, modular matrix, and topological characterization of other quantum states including the non-Abelian topological phase and the fractionalized states in TFB models with high Chern number ($C > 1$) in the future.

Acknowledgements. We thank Shoushu Gong for discussions. This work is supported by the US DOE Office

of Basic Energy Sciences under Grant No. DE-FG02-06ER46305 (DNS) and NSF under grants DMR-0906816 (WZ) and the Princeton MRSEC Grant DMR-0819860 (FDMH). DNS also acknowledges the travel support by the Princeton MRSEC.

[1] R. B. Laughlin, Phys. Rev. Lett. **50**, 1395 (1983).
[2] X. G. Wen, Phys. Rev. B **40**, 7387 (1989).
[3] F. D. M. Haldane, Phys. Rev. Lett. **61**, 2015 (1988).
[4] E. Tang, J. W. Mei and X. G. Wen, Phys. Rev. Lett. **106**, 236802 (2011).
[5] T. Neupert, L. Santos, C. Chamon and C. Mudry, Phys. Rev. Lett. **106**, 236804 (2011).
[6] K. Sun, Z. C. Gu, H. Katsura and S. Das Sarma, Phys. Rev. Lett. **106**, 236803 (2011).
[7] D. N. Sheng, Z. C. Gu, K. Sun and L. Sheng, Nature Commun. **2**, 389 (2011).
[8] Y.-F. Wang, Z.-C. Gu, C.-D. Gong and D. N. Sheng, Phys. Rev. Lett. **107**, 146803 (2011).
[9] N. Regnault and B. A. Bernevig, Phys. Rev. X **1**, 021014 (2011).
[10] B. A. Bernevig and N. Regnault, Phys. Rev. B **85**, 075128 (2012).
[11] Y. F. Wang, H. Yao, Z. C. Gu, C. D. Gong, and D. N. Sheng, Phys. Rev. Lett. **108**, 126805 (2012).
[12] Y. L. Wu, N. Regnault and B. A. Bernevig, Phys. Rev. Lett. **110**, 106802 (2013).
[13] M. Barkeshli and X.-L. Qi, Phys. Rev. X **2**, 031013 (2012).
[14] T. Scaffidi and G. Moller, Phys. Rev. Lett. **109**, 246805 (2012).
[15] D. Xiao, W. Zhu, Y. Ran, N. Nagaosa, and S. Okamoto, Nat. Commun. **2**, 596 (2011).
[16] G. Murthy and R. Shankar, Phys. Rev. B **86**, 195146 (2012).
[17] J. W. F. Venderbos, S. Kourtis, J. van den Brink, and M. Daghofer, Phys. Rev. Lett. **108**, 126405 (2012).
[18] Z. Liu and E. J. Bergholtz, Phys. Rev. B **87**, 035306 (2013).
[19] E. Kapit and E. Mueller, Phys. Rev. Lett. **105**, 215303 (2010).
[20] S. Yang, K. Sun and S. Das Sarma, Phys. Rev. B **85**, 205124 (2012).
[21] S. A. Parameswaran, R. Roy, and S. L. Sondhi, Phys. Rev. B **85**, 241308(R) (2012).
[22] X. G. Wen, Int. J. Mod. Phys. B **4**, 239 (1990).
[23] A. Kitaev and J. Preskill, Phys. Rev. Lett. **96**, 110404 (2006).
[24] M. Levin and X.-G. Wen, Phys. Rev. Lett. **96**, 110405 (2006).
[25] H. Li and F. D. M. Haldane, Phys. Rev. Lett. **101**, 010504 (2008).
[26] A. M. Lauchli, E. J. Bergholtz, J. Suorsa and M. Haque, Phys. Rev. Lett. **104**, 156404 (2010).
[27] H. C. Jiang, Z. H. Wang and L. Balents, Nat. Phys. **8**, 902 (2012).
[28] Y. Zhang, T. Grover, A. Turner, M. Oshikawa and A. Vishwanath, Phys. Rev. B **85**, 235151 (2012).
[29] L. Cincio and G. Vidal, Phys. Rev. Lett. **110**, 067208 (2013).
[30] M. P. Zaletel, R. S. K. Mong, and F. Pollmann, Phys. Rev. Lett. **110**, 236801 (2013).
[31] H. H. Tu, Y. Zhang, and X. L. Qi, arxiv:1212.6951.
[32] D. N. Sheng, X. Wan, E. H. Rezayi, K. Yang, R. N. Bhatt, and F. D. M. Haldane, Phys. Rev. Lett. **90**, 256802 (2003).
[33] S. Dong, E. Fradkin, R. G. Leigha and S. Nowling, JHEP 05, 016 (2008).
[34] E. Rowell, R. Stong, Z. H. Wang, Comm. Math. Phys. **292**, 343 (2009).
[35] P. Fendley, M. P. A. Fisher and C. Nayak, J.Stat.Phys. **126**, 1111(2007).
[36] T. Grover, arxiv:1112.2215.
[37] A. M. Lauchli, E. J. Bergholtz and M. Haque, New J. Phys. **12**, 075004 (2010).
[38] F. D. M. Haldane, Phys. Rev. Lett. **107**, 116801 (2011).
[39] B. Yang, Z. Papic , E. H. Rezayi, R. N. Bhatt, and F. D. M. Haldane, Phys. Rev. B **85**, 165318 (2012).